

RFI Sources, Identification, Mitigation (Part 2)

Mamoru Sekido/NICT

1 An Example of Serious RFI

1.1 Symptom

This is an example of very bad case a L-band receiver affected by RFI originated from ground base station of mobile phone. The NICT/Kashima Space Technology Center is operating 34m radio telescope (Kas34), which has several kinds of receivers (1.4-1.8GHz, 2.3GHz, 5GHz, 8.4GHz, 22GHz and 43GHz) for VLBI and single dish observations. Corresponding to the increased users of mobile phones, cellular carriers are not only increasing the number of base stations, but also expanding the use of radio frequency band and increasing transmission power of down-link communication. L-band(1.4-1.8GHz) and S-band(2.3GHz) are the frequency range, where these communications are using. Influence to radio astronomy is getting severer in these bands. Since NICT/Kashima is surrounded by residential area of Kashima city, it is not easy to prevent increases of cell-phone base stations. The nearest one located about 700m away from the Kas34 (Fig.1), and signals from these stations come into L-band receiver of Kas34 even the telescope is pointing to the zenith direction. The block diagram of the L-band receiver of the Kas34 is illustrated in Fig.2. Observation with the L-band receiver has been made at the radio astronomy protected band around 1420MHz, although the LNA has gain at wide frequency range of 1.4 - 1.9 GHz, thus the LNA could be saturated by a RFI at outside of the observation band. In this case, the most strong RFI signal comes in at 1480MHz. The RFI signal spectrum is displayed in left panel of Fig.3. Band-pass signal spectra of the

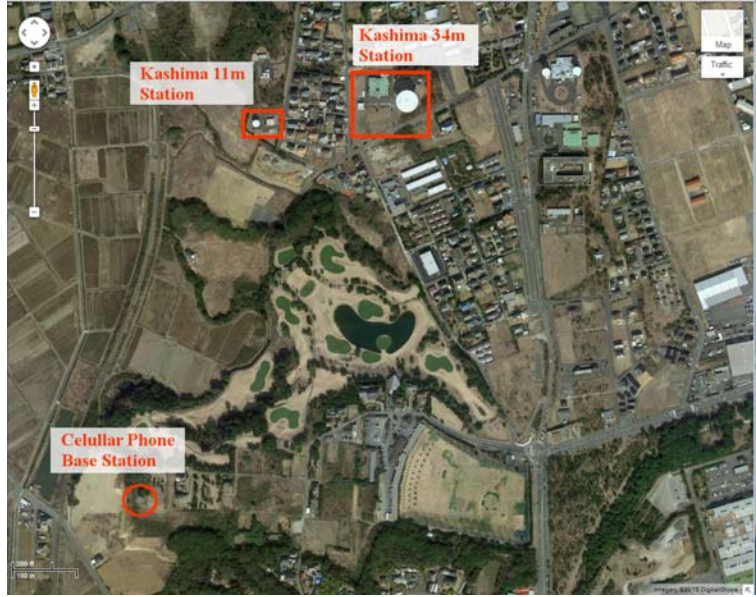


Figure 1: A map around the Kashima Space Technology Center (KSTC) is captured from Google Map. The positions indicated by square is the location of 34m and 11m telescopes. Marked by the circle is the nearest cell-phone base station to the KSTC.

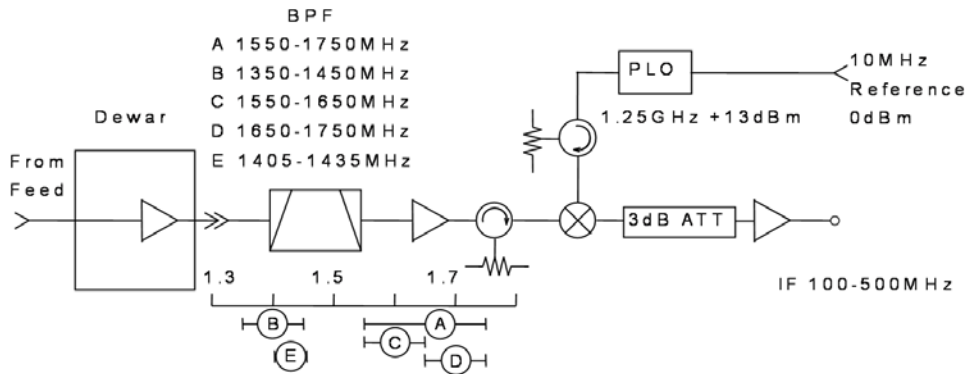


Figure 2: Block diagram of L-band receiver of 34m radio telescope. Observation used to be made by exchanging the bandpass filters (A-E), although RFI is getting severer to saturate the LNA sometimes.

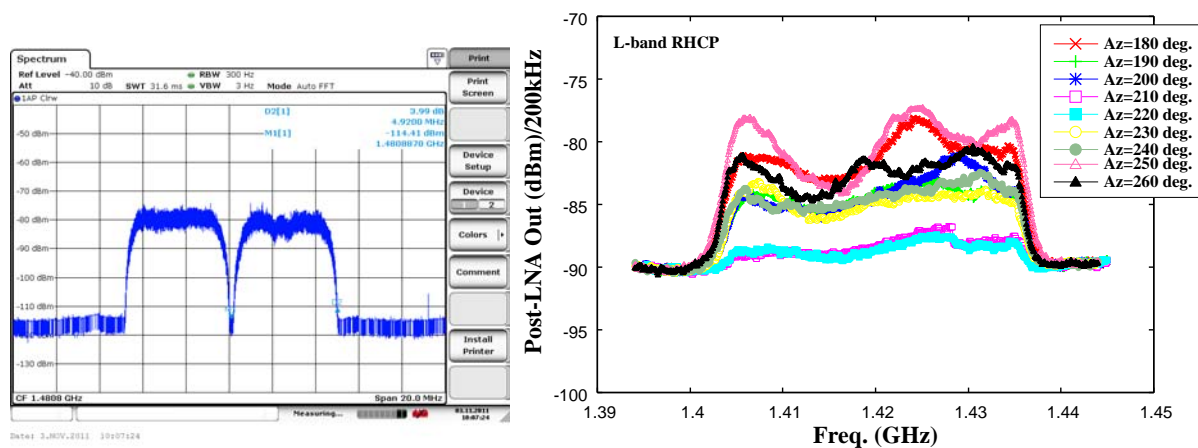


Figure 3: (Left) Frequency Spectrum of RFI signal at 1480MHz observed at LNA output of 34m radio telescope. (Right) A spectrum of the LNA output of 34m antenna L-band receiver in the direction (El = 7 deg., Az = 18-260 deg.). Received signal power fluctuation due to gain compression is observed in the direction Az = 210-220 deg., where cell phone base station is located.

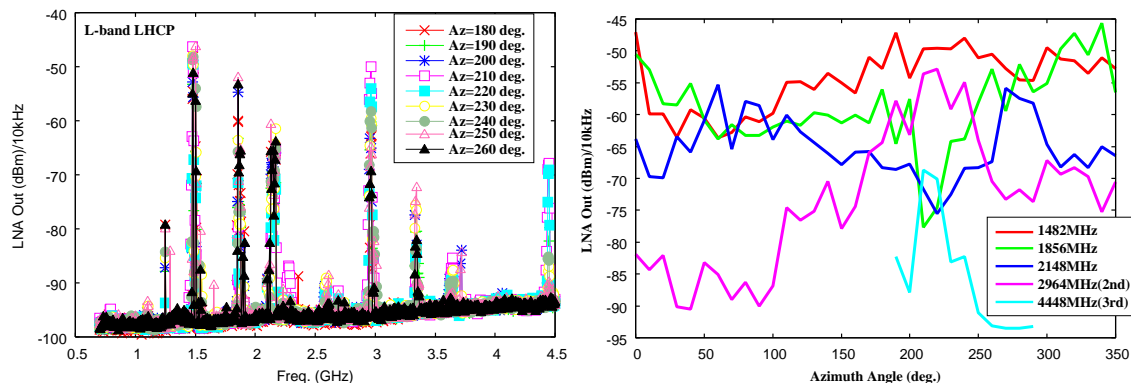


Figure 4: (Left) The second and third order harmonics of RFI (1480MHz) were observed from the spectrum of LNA output at EL = 7deg. Az = 180 - 260 deg. (Right) Power level of significant RFI signals are monitored as the function of Azimuthal angle, where EL=7 deg. Increases of 2nd and 3rd order harmonics of 1480MHz were observed at Az = 200-250 deg. The maximum ratio of 3rd order harmonics with respect to the fundamental signal(1480MHz) was about -20 dB.

LNA output are displayed in the right panel of Fig. 3. The gain compression due to the saturation of LNA is clearly seen in the data in direction of AZ = 210-220, where the cell phone base station is located.

1.2 Solution

For recovery of the receiver performance to the normal state, we have to understand how much attenuation have to be applied to the RFI signal. A parameter 'P1dB', which is defined by output power level of 1 dB gain compression, is widely used for indicator of the salutation level of amplifier. Although we did not have accurate value of P1dB parameter of our L-band LNA, nor measurement of the current input level of the RFI to the LNA is not easy because the LNA is inside the dewar in 15 Kelvin environment. Then we estimated the current input power level to LNA based on measurements of the ratio of 3rd order harmonics with respect to its fundamental wave. Fig.4 shows the measurement results of power level for each direction of azimuthal angle. It is clearly seen that the 2nd and 3rd order harmonics of 1480 MHz are increased around 210-220 deg. From this measurement, we got that the maximum ratio of the 3rd order harmonics to the fundamental wave (1480 MHz) was about -20 dB. The algorithm for estimation of input power level with respect to the P1dB level is explained in the appendix. Based on this measurement and theoretical consideration (see appendix), input power level with respect to the P1dB was estimated to be +3.2dB. Since

linear amplifier usually have to be used less than -10 dB from P1dB power level of the amplifier, requirement of the RFI attenuation is estimated to be more than 13.2 dB (=3.2 dB + 10 dB).

Since the frequency of the RFI signal at 1480MHz is out of the protected frequency band assigned for radio astronomy, we had no legal right to claim to the cell phone company, but thought a communication channel to the company at a radio frequency regulation committee meeting, I could make appointment and went to base station management division of the company. After explanation of the evidence of receiver saturation due to RFI and negotiation with them, we could agreed that the company will bear the expenses of installation of cryogenic filter in front of the LNA to prevent the saturation. The installation of cryogenic filter and recovery of the L-band receiver is expected to be made by the end of this year.

2 RFI Survey for development of wide-band VLBI System

2.1 Motivation

We are upgrading the MARBLE 1.5m/1.6m diameter antennas to wide-band (VLBI2010 compatible) VLBI system. The MARBLE antennas are originally developed for baseline calibration/validation for GNSS receivers under the collaboration with Geographical Survey Institute (GSI) of Japan. S/X-band receivers have been installed in these antennas, though it designed with future extension to wide-band (VLBI2010) specification in mind. Then we have made a RFI survey to check the feasibility of wide-band observation and location of RFI signal, before modification of the MARBLE to wide-band system.

VLBI is relatively robust to the RFI, because local RFI signals are independent each other and it will diminish in cross correlation processing, as far as it is not strong to overload the receiver system. However RFI signal originated from communication use are usually strong enough with respect to the power level of radio astronomy observation. It can easily overload the dynamic range of the cascaded amplifiers from front end to the recording system. Table 1 shows an example of signal power level and gain of a radio telescope. Because of large gain about 90 dB and limited dynamic range, receiver system could be saturated by strong RFI signal in the observation band.

Especially, due to wide observation frequency band of VLBI2010 specification, the receiver is more vulnerable to RFI and higher P1dB performance is required for the amplifiers. Measurements of RFI signal power level with respect to that of receiver noise is useful.

Table 1: An example of signal power level and gain of a typical radio telescope.

Typical Signal level at LNA input.	100	Kelvin
	1.38e-18	mW/Hz
(signal level in 1Hz Band width)	-179	dBm/Hz
(signal level in 500MHz Band width)	-91	dBm/500MHz
Amplifier Gain	90	dB
Typical Sampler input level	0	dBm
Dynamic range of a 8bit A/D sampler (8 bit = 256 levels)	24	dB

2.2 Receiver system and its noise temperature used for the RFI survey.

Portable wide-band receiver (2-18GHz), which was developed in the project “Statistical approach for weak radiation power measurement in radio frequency (SIRIUS)” was used in the radio environment survey. The SIRIUS receiver has been sometimes suffered from very strong interference below 3 GHz band, then we decided to introduce high-pass filter (HPF:Fc=3.5GHz) in front of LNA. Therefore This report does not include the RFI information below 3 GHz.

Before the RFI survey, noise temperature of the SIRIUS+HPF receiver with taking into account of the insertion loss of HPF and loss of feed system DRH(Double Ridged Horn) antenna, Schwarzbeck BBHA-9120D) was evaluated at first. The Main equipment used for the measurement is displayed in Fig. 5. Schematic diagram and pictures are displayed in Fig. 6.

As indicated in the Fig.6, three ways of measurements were performed to get receiver noise temperature and system noise temperature.

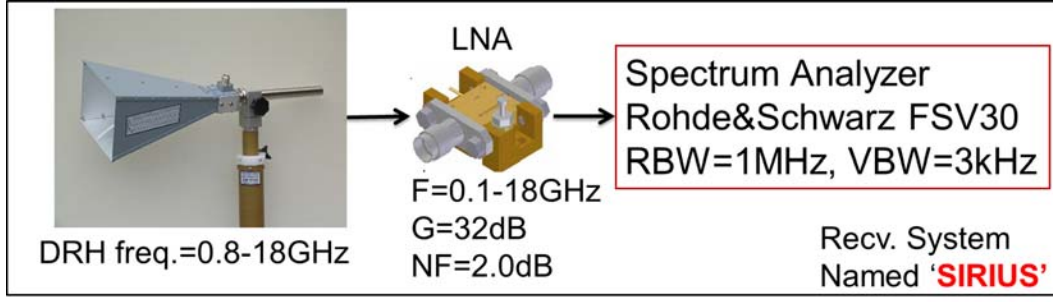


Figure 5: Antenna and LNA used for the RFI survey.

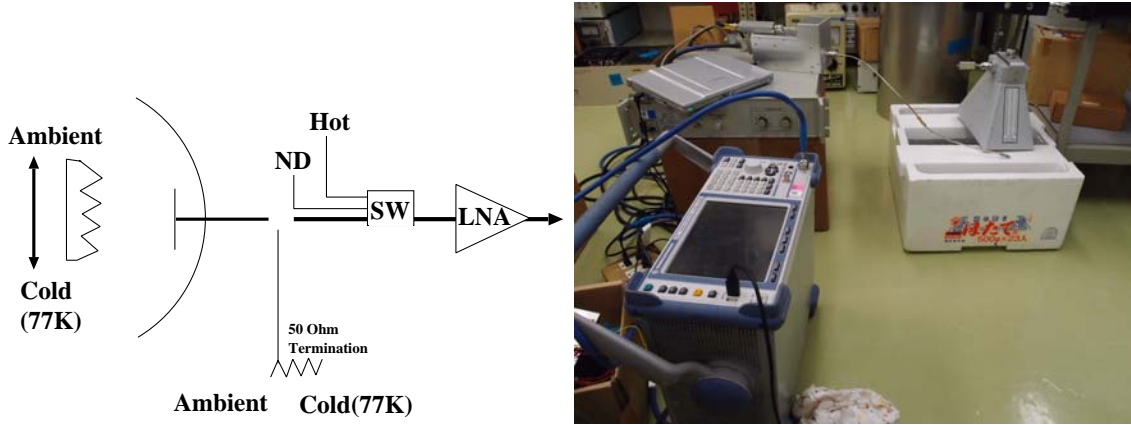


Figure 6: Schematic diagram of receiver temperature measurement (Left panel), and a picture of the equipment (Right panel). LNA inputs can be selected one of the noise diode(ND), 50 ohms terminator in room temperature (Hot), and antenna output. In the measurement of receiver (LNA) noise temperature, antenna output was replaced with 50 ohms terminator in liquid nitrogen (77K) connected via semi-rigid cable. For measurement of system noise temperature including DRH antenna, radio wave absorber in room temperature (300K) and that in liquid nitrogen (77K) were compared.

1. At the LNA input port, hot load and noise diode, whose noise power is known, were switched. Then receiver noise temperature (T_{rx1}) was computed from their ratio of their power levels.

$$Y_1 \equiv \frac{P_{ND}}{P_{HOT}} = \frac{T_{rx} + T_{ND}}{T_{rx} + T_{HOT}} \quad (1)$$

$$T_{rx,1} \equiv \frac{T_{ND} + Y_1 \cdot T_{HOT}}{Y_1 - 1} \quad (2)$$

2. By switching the LNA input ports to 50 ohms termination in room temperature (Hot) and to that in liquid nitrogen (77K), receiver output was measured. Then receiver noise temperature (T_{rx2}) was computed from their ratio of their power levels.

$$Y_2 \equiv \frac{P_{HOT}}{P_{COLD}} = \frac{T_{rx} + T_{HOT}}{T_{rx} + T_{COLD}} \quad (3)$$

$$T_{rx,2} \equiv \frac{T_{HOT} + Y_2 \cdot T_{COLD}}{Y_2 - 1} \quad (4)$$

3. By comparing the receiver power outputs from DRH antenna with antenna aperture covered with absorber in room temperature, and that in liquid nitrogen, the system noise temperature including the antenna (T'_{rx}) was computed from their ratio.

$$Y_3 \equiv \frac{P_{HOT}}{P_{COLD}} = \frac{T_{rx} + \alpha \cdot T_{HOT} + (1 - \alpha)T_{amb}}{T_{rx} + \alpha \cdot T_{COLD} + (1 - \alpha)T_{amb}} = \frac{T_{HOT} + T'_{rx}}{T_{COLD} + T'_{rx}} \quad (5)$$

$$T'_{rx} \equiv \frac{T_{HOT} + Y_3 \cdot T_{COLD}}{Y_3 - 1} \quad (6)$$

where, α indicate the loss factor due to the HPF and the DRH antenna. We assumed ambient temperature T_{amb} is the same with temperature of hot load $T_{amb} \simeq T_{HOT}$.

T'_{rx} in equation (6) is system temperature including the antenna. Signal transmission loss α in front of LNA contributes to the increase of receiver temperature $1/\alpha$ times as

$$T'_{rx} = \frac{(1 - \alpha)T_{amb} + T_{rx}}{\alpha}, \quad (7)$$

where T_{amb} is ambient temperature, and T_{rx} is original receiver noise temperature of LNA.

Measurement results of receiver noise temperature by Y-factor method is indicated in Fig. 7. T_{rx2} computed from 'Hot-Cold(77K)' is must be close to the the real receiver noise temperature (T_{rx}) including microwave switch. T'_{rx} (Hot-Cold(77K with Horn)) is higher than T_{rx2} at lower (≤ 3 GHz) frequency. That is because of insertion loss of the HPF and loss of the antenna.

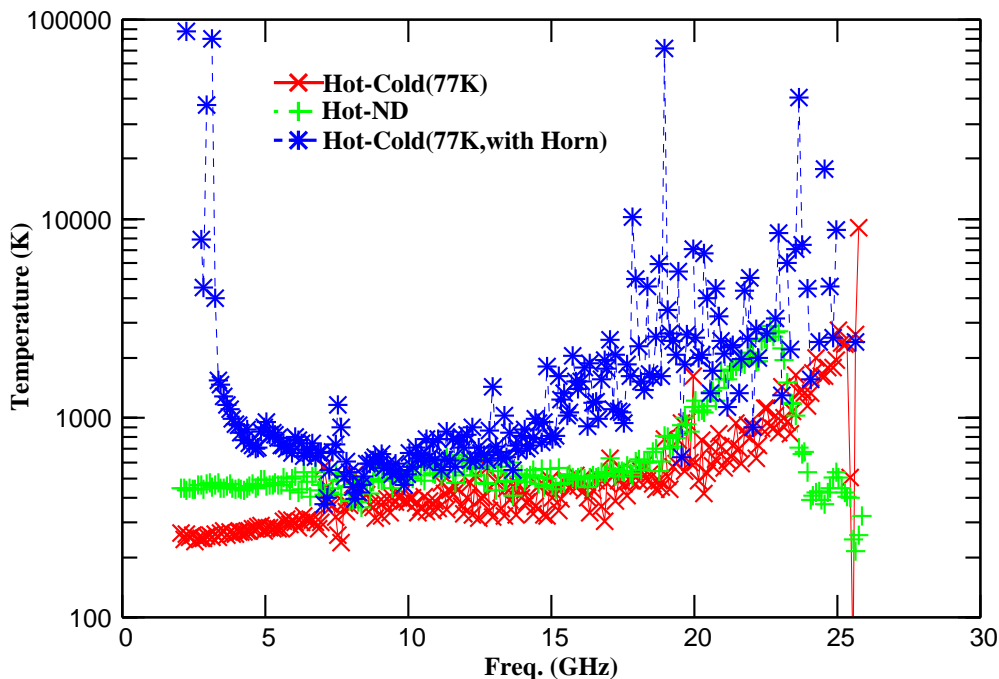


Figure 7: Receiver noise temperatures measured by three ways. 'Hot-Cold(77K)', 'Hot-ND', and 'Hot-Cold(77K,with Horn)' correspond to T_{rx2} , T_{rx1} , and T_{rx} of equation (2),(4),(6) in the text respectively. Note that 'Hot-ND' is derived based on noise diode power of nominal values rather than measurement. Then 'Hot-Cold(77K)' is thought to be close to real receiver temperature including microwave switch. System noise temperature T'_{rx} (Hot-Cold(77K with Horn)) is higher at lower (≤ 3 GHz) and higher (≥ 15 GHz) because of insertion loss of HPF and loss of the antenna.

2.3 RFI Survey and Results

Wide band receiver system developed in the project "Statistical approach for weak radiation power measurement in radio frequency (SIRIUS)", which is composed of double-ridged horn (DRH) antenna(Schwarzbeck BBHA-9120D) and wide band low noise amplifier (LNA), was used for this RFI survey. The receiver has capable to observe radio signal 2 – 18 GHz frequency range, and its output was recorded with spectrum analyzer (Rohde Schwartz FSV: 0-30GHz).

Table 2: RFI Measurement conditions and Parameters

Measurement Method	Max Hold
Polarization	Linear(V,H)
Max Hold Duration	30 sec.
RBW	1 MHz
VBW	1 MHz
Observation direction	Horizontal direction to East/South/West/North, and Zenith



Figure 8: Picture of the measurement locations: (A) Left: At the roof of Kashima-34m-antenna operation building. (B) Center: At the roof of operation building of Koganei 11m station, (C)Right: At the roof of National Metrology Institute of Japan(NMIJ) building.

Because RFI signal was too strong below 3 GHz-band to saturate the receiver system, we introduced high-pass filter (HPF: $F_c=3.5\text{GHz}$) for measurement in front of LNA input to prevent saturation of the system.

The RFI surveys were performed at three locations: (A) the roof of Kashima-34m antenna operation building(NICT Space Technology Center, Kashima), (B) at the roof of operation building of Koganei 11m station (Koganei Headquarter of NICT, Tokyo), and (C) at the roof of National Metrology Institute of Japan (NMIJ) building (Tsukuba). View of the survey sites are displayed in Fig.8. Measurement mode of Max Hold function of spectrum analyzer (Rohde Schwartz FS-V) was used for 30 seconds to take a data for one direction of the sky. Measurement parameters are listed in Table 2. In the latter section, intensity of received radio signal is expressed with unit of temperature of black body radiation. Please aware that this is based on the assumption: signal amplitude distribution obeys Gaussian probability distributions. Although signal power distribution is not always Gaussian for the artificial RFI, thus the expression in temperature is an approximation.

Then mean power level must be used to express the radiation power in temperature. 'Max Hold' measurement is recording of the maximum power level received during the specified period. Thus 'Max Hold' measurement result does not always proportional to the mean of the power, though here we assume that (1) 'Max Hold' measurement value obtained by sufficiently long period of accumulation is proportional to the mean power level. Additionally (2) radiation power distribution of RFI is the same with that of black-body radiation. Based on these assumption, ratios of Max Hold measurement results of Noise diode (P_{ND}), Hot-load (P_{Hot}), and antenna (P_{Ant}) are expressed as

$$Y_1 = \frac{P_{ND}}{P_{Hot}} = \frac{T_{rx} + T_{ND}}{T_{rx} + T_{Hot}} \quad (8)$$

$$Y_2 = \frac{P_{Sky}}{P_{Hot}} = \frac{T_{rx} + T_{Sky}}{T_{rx} + T_{Hot}}, \quad (9)$$

where T_{Hot} and T_{rx} are noise temperature of noise diode and Hot-load temperature, respectively. Then receiver temperature (T_{rx}) and antenna temperature (T_{Sky}) are given by the unit of Kelvin by following equations.

$$T_{rx} = \frac{T_{ND} + Y_1 \cdot T_{Hot}}{Y_1 - 1} \quad (10)$$

$$T_{Sky} = Y_2 \cdot (T_{rx} + T_{Hot}) - T_{rx}. \quad (11)$$

Radio signal power spectra received (V-Linear Polarization) in the environment at location (A),(B),and (C) are indicated in Fig. 9, Fig.10, and Fig.11 where power level was converted to temperature expression via equation (11).

2.4 RFI Sources

Followings can be the source of RFI. The RFI environment may differ from country to country, because that depends on the government radio regulation policy. Following is the case of Japan.

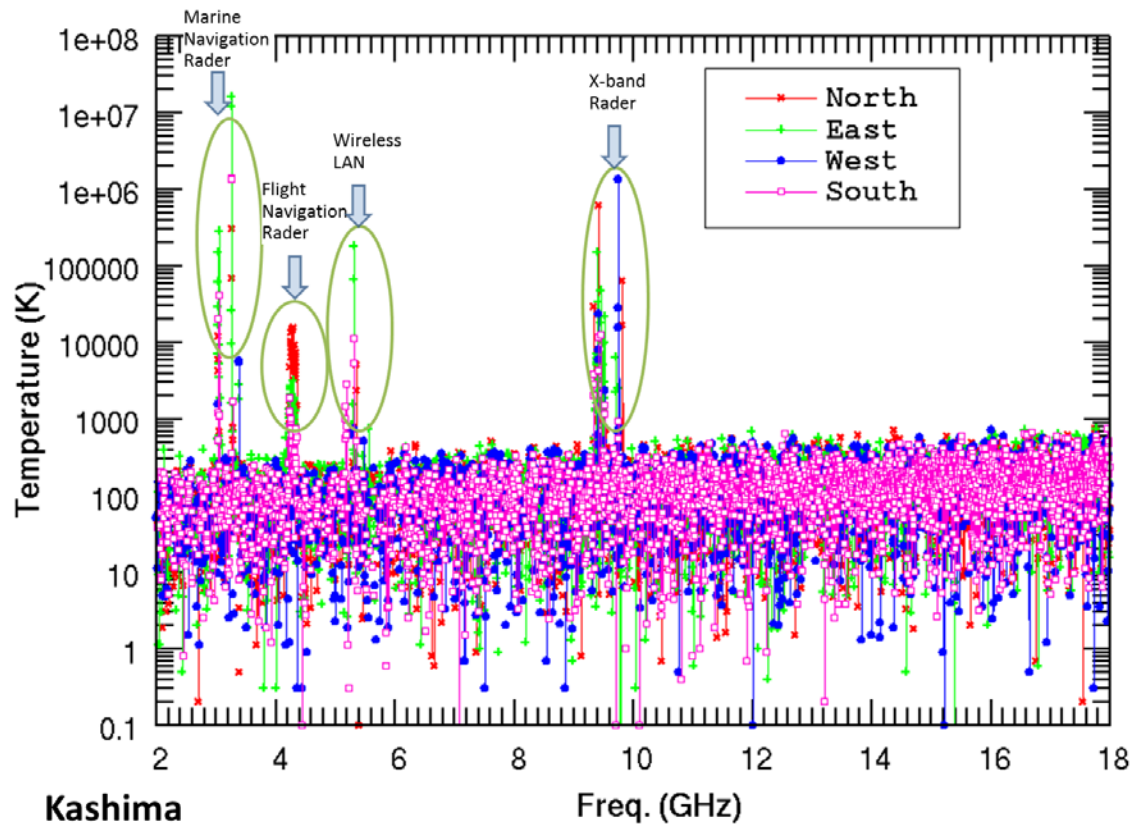


Figure 9: Radio signal spectrum received at location (A) Roof of Kashima 34m antenna operation building. Power level of the signal is indicated with noise temperature.

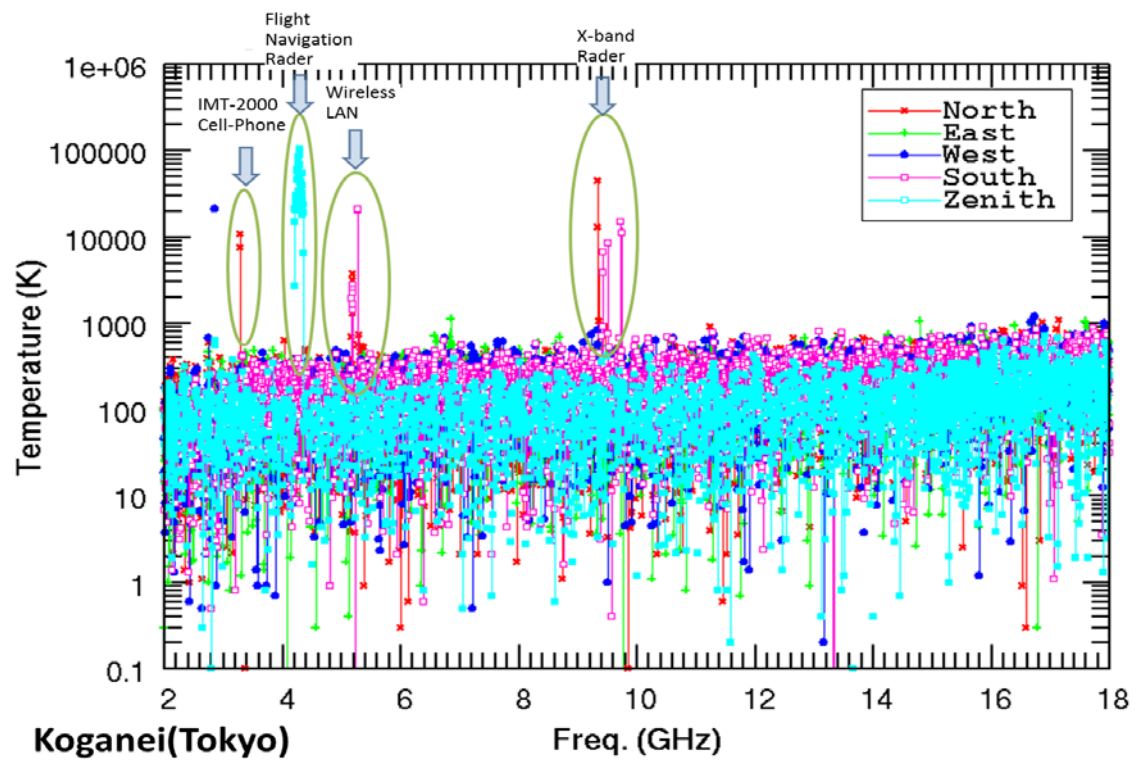


Figure 10: Radio signal spectrum received at location (B) Roof of Koganei 11m antenna operation building at NICT headquarter. Power level of the signal is indicated with noise temperature.

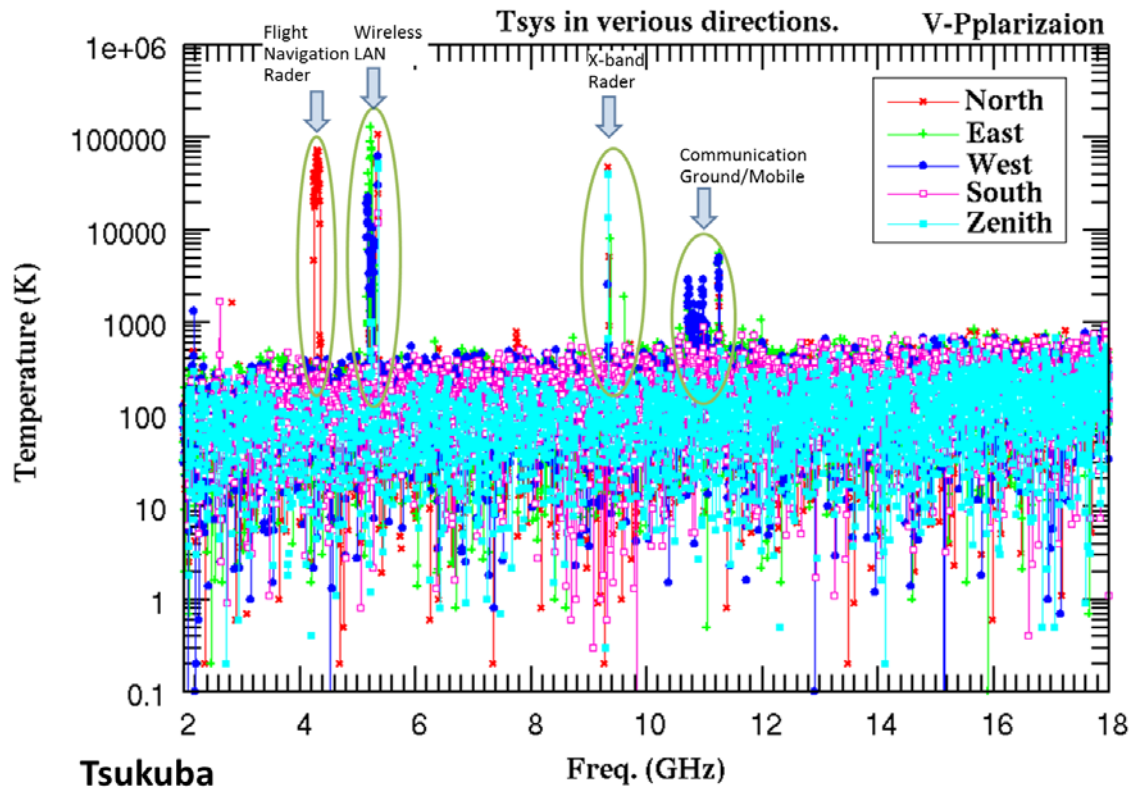


Figure 11: Radio environment observed at location (C) roof of NMIJ building in vertical linear polarization.

1. Cell phone and its base station. (1.48GHz 1.9GHz, 2.2GHz)
2. 3.0 - 3.4 GHz: Marine Navigation Rader
3. 4.25-4.35 GHz: Flight Navigation Rader (Altimeter)
4. 5.15-5.35 GHz: Wireless LAN
5. 9.35-9.45, 9.7-9.8 GHz: X-band Rader (Weather, Marine)
6. 11.7-12.2 GHz: Broadcasting Satellite
7. 12.2-12.75 GHz: Communication Satellite

Based on the radio regulation assignment table provided from the ministry of general affairs of Japan, sources of RFI detected in the RFI survey are estimated and indicated in the Fig. 9, 10, and 11.

A Appendix: Estimation of RFI level w.r.t. the P1dB level of the LNA.

Class-A amplifiers are used for small signal amplification in radio astronomy receiver system, and its linearity between input and output signal is important. However, gain of amplifier is compressed and amplifier's response deviates from linear relation when input signal become larger than a certain level of power. Clipping of amplitude of output signal causes mixing (inter-modulation) of the signals. The **P1dB** and Third Order Intercept Point (TOI or IP3) are the amplifier's performance parameters, which indicates the power level of transition from linear response region to the saturation region. This section reminds the relation between P1dB and IP3[1]. And estimate the current input signal level with respect to the P1dB of the amplifier based on a measurement of power ratio of 3rd order harmonics to the fundamental wave.

A.1 P1dB level

An amplifier's response including non-linearity is express with as a relation between input voltage v_i and output voltage v_o as:

$$v_o = k_1 v_i + k_2 v_i^2 + k_3 v_i^3 + \dots \quad (12)$$

When input signal is $v_i = A \cos \omega t$, output signal is expressed with up to the 3rd order term as

$$\begin{aligned} v_o &= k_1 A \cos \omega t + k_2 A^2 \cos^2 \omega t + k_3 A^3 \cos^3 \omega t \\ &= k_1 A \cos \omega t + k_2 A^2 \left(\frac{1}{2} + \frac{1}{2} \cos 2\omega t \right) + k_3 A^3 \left(\frac{3}{4} \cos \omega t + \frac{1}{4} \cos 3\omega t \right) \\ &= \frac{1}{2} k_2 A^2 + \left(k_1 A + \frac{3}{4} k_3 A^3 \right) \cos \omega t + \frac{1}{2} k_2 A^2 \cos 2\omega t + \frac{1}{4} k_3 A^3 \cos 3\omega t. \end{aligned} \quad (13)$$

The Gain (G_{NL}) of the fundamental wave in the non-linear region is expressed as

$$G_{\text{NL}} = 20 \log \frac{k_1 A + \frac{3}{4} k_3 A^3}{A} = 20 \log \left(k_1 + \frac{3}{4} k_3 A^2 \right) \quad (14)$$

and the gain (G) in linear region is derived with $k_3 = 0$ as

$$G = 20 \log k_1. \quad (15)$$

Gain of fundamental wave is compressed in non-linear region, this means $G_{\text{NL}} < G$, thus $k_3 < 0$ is derived.

The **P1dB** is defined as a output power level, where the gain is compressed by 1 dB with respect to the gain in linear region. Thus the gain at **P1dB** is $G_{1\text{dB}} = G - 1$ [dB]. This means gain at P1dB is 0.89125 of that in linear region. Then the expression of input signal amplitude at P1dB ($A_{1\text{dB}}$) is derived with the relation $0.89125 k_1 = k_1 + \frac{3}{4} k_3 A_{1\text{dB}}^2$ as

$$A_{1\text{dB}}^2 = 0.145 \frac{k_1}{|k_3|}. \quad (16)$$

An expression of input power [dBm] with voltage amplitude and impedance $Z_0 = 50\Omega$ is given as

$$P_{\text{in}} = 10 \log \left[\left(\frac{A}{\sqrt{2}} \right)^2 \frac{1000}{Z_0} \right]. \quad (17)$$

Substituting equation (16), output power at **P1dB** is expressed with coefficients of fundamental wave k_1 and third harmonics k_3 as

$$P_{1\text{dB}} = G - 1 + P_{\text{in}} = 10 \log k_1^2 - 1 + 10 \log \left[\frac{0.145 k_1}{2 |k_3|} 20 \right] = 10 \log \frac{k_1^3}{|k_3|} + 0.6137 [\text{dBm}]. \quad (18)$$

A.2 Two tone signal analysis: IP3 or TOI

Let's suppose two signals (angular frequency ω_1 and ω_2) are fed into an amplifier. Substitution of a input signal q

$$v_i = B (\cos \omega_1 t + \cos \omega_2 t)$$

into equation (12) gives expression of output signal with up to 3rd order terms as

$$\begin{aligned} v_o &= k_1 B (\cos \omega_1 t + \cos \omega_2 t) + k_2 B^2 (\cos \omega_1 t + \cos \omega_2 t)^2 + k_3 B^3 (\cos \omega_1 t + \cos \omega_2 t)^3 \\ &= k_2 B^2 + k_2 B^2 \cos(\omega_1 - \omega_2)t + \left(k_1 B + \frac{9}{4} k_3 B^3\right) \cos \omega_1 t + \left(k_1 B + \frac{9}{4} k_3 B^3\right) \cos \omega_2 t \\ &\quad + \frac{3}{4} k_3 B^3 \cos(2\omega_1 - \omega_2)t + \frac{3}{4} k_3 B^3 \cos(2\omega_2 - \omega_1)t + k_2 B^2 \cos(\omega_1 + \omega_2)t \\ &\quad + \frac{1}{2} k_2 B^2 \cos 2\omega_1 t + \frac{1}{2} k_2 B^2 \cos 2\omega_2 t + \frac{3}{4} k_3 B^3 \cos(2\omega_1 + \omega_2)t + \frac{3}{4} k_3 B^3 \cos(2\omega_2 + \omega_1)t \\ &\quad + \frac{1}{4} k_3 B^3 \cos^3 \omega_1 t + \frac{1}{4} k_3 B^3 \cos^3 \omega_2 t. \end{aligned} \quad (19)$$

The second order inter-modulation (SOI) generates the frequency $(\omega_1 \pm \omega_2)$, and third order inter-modulation (TOI) generates frequency $(2\omega_1 \pm \omega_2)$ and $(2\omega_2 \pm \omega_1)$. When two frequencies are close ($\omega_1 \cong \omega_2$) and the amplifier has narrow frequency response, signal other than $\omega_1, \omega_2, 2\omega_2 - \omega_1$, and $2\omega_1 - \omega_2$ are suppressed.

From the coefficient of equation (19), the power of fundamental wave and 3rd order harmonics are expressed as

$$P_0 = 10 \log \left[\left(\frac{k_1 B}{\sqrt{2}} \right)^2 \frac{1000}{Z_0} \right] \quad (20)$$

$$P_{\omega_1} = 10 \log \left[\left(k_1 B + \frac{9}{4} k_2 B^2 \right)^2 \frac{1000}{2Z_0} \right] \quad (21)$$

$$P_{2\omega_1 - \omega_2} = 10 \log \left[\left(\frac{3}{4} k_3 B^3 \right)^2 \frac{1000}{2Z_0} \right]. \quad (22)$$

The **IP3** (Third order intercept point) is a virtual power level defined as the third order harmonics power is equal with power of fundamental wave $P_0 = P_{2\omega_1 - \omega_2}$. By comparing equations (20) and (22), $k_1 B = \frac{3}{4} k_3 B^3$ is derived. Then amplitude of input signal at IP3 level is given as

$$B_{\text{IP3}}^2 = \frac{4}{3} \frac{k_1}{|k_3|}. \quad (23)$$

Therefore output power of 3rd order harmonics P_{IP3} is obtained by substituting equation (23) into equation (22) as

$$P_{\text{IP3}} = 10 \log \left[\frac{2k_1^3}{3|k_3|} \frac{10^3}{Z_0} \right] = 10 \log \frac{k_1^3}{|k_3|} + 11.249 \text{ dBm} \quad (24)$$

By taking difference with equation (18),

$$P_{\text{IP3}} - P_{\text{1dB}} = 10.635 \text{ dBm}. \quad (25)$$

This shows the well-known relation that output power level difference between IP3 and P1dB is about 10 dB. At this point, input power level difference between IP3 and P1dB is given as

$$\left(\frac{B_{\text{IP3}}}{A_{\text{1dB}}} \right)^2 = \frac{4k_1}{3|k_3|} \times \frac{|k_3|}{0.145k_1} = 9.195 \text{ (9.64dB) }. \quad (26)$$

A.3 The ratio between P_1 and P_3

In practical condition, we can measure the ratio between output power of fundamental wave and that of 3rd order harmonics, but power level measurement of first LNA input is difficult. When both a amplifier's P1dB

level and its input power level is unknown, we have to estimate the current input power level with respect to the P1dB of the amplifier.

When single tone signal is input, the output power ration between fundamental wave and 3rd order harmonics is expressed with the coefficient of the equation (13) as

$$R_{13} \equiv \frac{P_3}{P_1} = \left(\frac{\frac{1}{4}k_3A^3}{k_1A + \frac{3}{4}k_3A^3} \right)^2 = \left(\frac{\frac{|k_3|}{k_1}A^2}{4 - 3\frac{|k_3|}{k_1}A^2} \right)^2 \quad (27)$$

$$\sqrt{R_{13}} = \frac{\alpha\left(\frac{A}{A_{1dB}}\right)^2}{4 - 3\alpha\left(\frac{A}{A_{1dB}}\right)^2}, \quad (28)$$

where $\alpha \equiv 0.145$ and equation(16) were used. The first equation represent the power ratio and the second equation express the amplitude ratio with the amplitude of **P1dB** level. Then the ratio of current input power level with respect to the P1dB input level is expressed by

$$\left(\frac{A}{A_{1dB}} \right)^2 = \frac{4\sqrt{R_{13}}}{\alpha(1 + 3\sqrt{R_{13}})}. \quad (29)$$

In the case of L-band receiver of Kashima 34m radio telescope, the ratio R_{13} at (Az=210-220 deg., El=7deg) was about -20 dB (Fig. 4). Substituting $R_{13} = -20$ dB into equation (29) yield $\left(\frac{A}{A_{1dB}} \right)^2 = 2.12$ (+3.2dB). Thus current RFI input level is estimated to be +3.2 dB stronger than P1dB input level.

References

- [1] Inder J. Bahl, "Fundamentals of RF and Microwave Transistor Amplifiers", Wiley Publication., ISBN: 978-0-470-46231-7, 2009.